Free Radical Biology & Medicine 45 (2008) 32–39

Contents lists available at ScienceDirect

Free Radical Biology & Medicine

journal homepage: www.elsevier.com/locate/freeradbiomed

Original Contribution

Immunolocalization and enzymatic functional characterization of the thioredoxin system in *Entamoeba histolytica*

Diego G. Arias [a,b], Pedro G. Carranza [c,d], Hugo D. Lujan [c,d], Alberto A. Iglesias [b], Sergio A. Guerrero [a,*]

[a] *Laboratorio de Bioquímica Microbiana, Facultad de Bioquímica y Ciencias Biológicas, Universidad Nacional del Litoral, Ciudad Universitaria–Paraje El Pozo, 3000 Santa Fe, Argentina*
[b] *Laboratorio de Enzimología Molecular, Facultad de Bioquímica y Ciencias Biológicas, Universidad Nacional del Litoral, Ciudad Universitaria–Paraje El Pozo, 3000 Santa Fe, Argentina*
[c] *INIMEC-CONICET, Argentina*
[d] *Facultad de Cs. Médicas, Universidad Católica de Córdoba, Argentina*

ARTICLE INFO

Article history:
Received 6 November 2007
Revised 18 February 2008
Accepted 2 March 2008
Available online 20 March 2008

Keywords:
Thioredoxin
Entamoeba histolytica
Redox balance
Peroxiredoxin
Thiols

ABSTRACT

The components of the redox metabolism in *Entamoeba histolytica* have been recently revisited by Arias et al. (*Free Radic. Biol. Med.* 42:1496–1505; 2007), after the identification and characterization of a thioredoxin-linked system. The present work deals with studies performed for a better understanding of the localization and identification of different components of the redox machinery present in the parasite. The gene encoding for amoebic thioredoxin 8 was cloned and the recombinant protein typified as having properties similar to those of thioredoxin 41. The ability of these thioredoxins and the specific reductase to assemble a system utilizing NADPH to metabolize hydroperoxides in association with a peroxiredoxin has been kinetically characterized. The peroxiredoxin behaved as a typical 2 cysteine enzyme, exhibiting a ping-pong mechanism with hyperbolic saturation kinetics for thioredoxin 8 (K_m = 3.8 μM), thioredoxin 41 (K_m = 3.1 μM), and *tert*-butyl hydroperoxide (K_m about 35 μM). Moreover, the tandem system involving thioredoxin reductase and either thioredoxin proved to be operative for reducing low molecular weight disulfides, including putative physiological substrates as cystine and oxidized trypanothione. Thioredoxin reductase and thioredoxin 41 (by association also the functional redox system) have been immunolocalized underlying the plasma membrane in *Entamoeba histolytica* cells. These findings suggest an important role for the metabolic pathway involving thioredoxin as a redox interchanger, which could be critical for the maintenance and virulence of the parasite when exposed to highly toxic reactive oxygen species.

© 2008 Elsevier Inc. All rights reserved.

Introduction

Amoebiasis is an intestinal infection widespread throughout the world and caused by the human pathogen *Entamoeba histolytica*. The parasitic disease is the third leading cause of death in almost all countries where sewage and water quality are inadequate [1–3], causing 50 million clinical episodes of dysentery or amoebic liver abscess and ca. 100,000 deaths annually [4,5]. Identification and functional characterization of molecular targets are relevant matters for the rational design of new therapeutic drugs, which could improve the treatment of the disease [3,5–11]. In this regard, processes involved in redox metabolism are of particular interest in *E. histolytica* [7–11].

We have recently reported [12] the molecular cloning of two genes from *E. histolytica* encoding for thioredoxin reductase (*Eh*TRXR) and thioredoxin 41 (*Eh*TRX41), followed by their expression, purification, and functional characterization of the recombinant proteins. After these findings, the metabolic redox scenario operative in *E. histolytica* was revisited and the occurrence of a system (the *Eh*TRXR/TRX system) operating with a two cysteines peroxiredoxin (*Eh*p29; now more properly abbreviated *Eh*2CysPrx) has been proposed [12]. This metabolic pathway is complemented with other components such as Fe-superoxide dismutase (Fe-SOD), rubrerythrin, cysteine, flavoprotein A, and a 34-kDa oxidoreductase (*Eh*p34) [13]. In addition, it has been established that *E. histolytica* lacks or has insignificant amounts of glutathione and its associated enzymes [14,15], with cysteine being the major intracellular thiol [15,16]. Another metabolite reported to be present in *E. histolytica* is trypanothione [N^1,N^8-bis-(gluthationyl)-spermidine] [8,11,17], a thiol compound that in trypanosomatids is involved in the detoxification of reactive oxygen species, and alternatively can transfer reduction equivalents to TRX as well [18].

It is of relevance to further characterize the *Eh*TRXR/TRX system, especially with respect to the identification of all of its components, its cellular localization, kinetic properties, and the identification of different associated metabolites. This in-depth study is a prerequisite to a better understanding of the functionality of the redox system

* Corresponding author. Fax: +54 342 457 5221.
E-mail address: sguerrer@fbcb.unl.edu.ar (S.A. Guerrero).

Abbreviations: BSA, bovine serum albumin; IPTG, isopropyl-β-D-thiogalactopyranoside; PBS, phosphate-buffered saline; PCR, polymerase chain reaction; SDS-PAGE, sodium dodecyl sulfate-polyacrylamide gel electrophoresis; SOD, superoxide dismutase; TS_2, trypanothione.

0891-5849/$ – see front matter © 2008 Elsevier Inc. All rights reserved.
doi:10.1016/j.freeradbiomed.2008.03.008

when the parasite is challenged under oxidative stress conditions. We present herein the cellular localization of *Eh*TRXR and *Eh*TRX41 in *E. histolytica* trophozoites, together with a kinetic study of *Eh*2CysPrx. In addition, we identify TRX8 as another component that is able to work together with TRXR, after having properties similar to those of TRX41. We also characterize the NADPH-dependent activity of the system associated with the reduction of low molecular weight disulfides, metabolites that are thought to be critical for maintaining a reduced intracellular redox potential [15,16]. The present study reinforces the view that the *Eh*TRXR/TRX system is a key molecular target for the design of new therapeutic drugs for amoebiasis.

Materials and methods

Materials

Bacteriological media components were from Britania Laboratories (Rosario, Argentina). All other reagents and chemicals were of the highest quality commercially available.

E. histolytica cultivation

Trophozoites of *E. histolytica* strain HM1:IMSS were axenically cultured at 36.5 °C in TYI-S-33 medium supplemented with 12% heat-inactivated adult bovine serum and 2% Diamond's vitamin [19].

Molecular cloning of trx8 from E. histolytica

The gene was amplified by PCR using *E. histolytica* genomic DNA as a template and primers designed after spliced sequences reported in the Wellcome Trust, Sanger Institute, Pathogen Sequencing Unit: http://www.genedb.org/. The specific primers were TRX8Fow, 5′-GGATCCATGGCTGTACTTCATATTAAC-3′; and TRX8Rev, 5′-AAGCTTTTATGCTGTTTCAACCATTTG-3′. The PCR was performed under the following conditions: 94 °C for 10 min; 30 cycles of 94 °C for 1 min, 55 °C for 1 min, and 72 °C for 1 min, and then 72 °C for 10 min. The PCR product was subsequently purified and ligated into the pGEM-T Easy vector (Promega) to facilitate further work. The fidelity and correctness of the gene were confirmed on both strands by complete sequencing. The construct and the pRSET-A vector (Invitrogen) were digested with *Bam*HI and *Hind*III. Ligation to the pRSET-A vector of the insert was performed using T4 DNA ligase for 16 h at 16 °C. Preparation of plasmid DNA and subsequent *Bam*HI/*Hind*III restriction treatment were performed to check the correctness of the different constructs.

Expression and purification

*Eh*TRXR, *Eh*TRX8, *Eh*TRX41, and *Eh*2CysPrx were expressed in *Escherichia coli* as His-tag (N-terminal) recombinant proteins, and chromatographically purified as previously described [12]. Briefly, single colonies of *E. coli* BL21(DE3) transformed with the respective recombinant plasmid were selected. Overnight cultures were diluted 1/100 in fresh media (LB broth supplemented with 100 μg/ml ampicillin) and grew under identical conditions to the exponential phase, OD_{600} of 0.6. The expression of the recombinant proteins was induced with 0.5 mM IPTG, followed by incubation at 28 °C. After 16 h the cells were harvested and stored at -20 °C. Purification was performed using a Co^{2+}-IDA-agarose resin (Invitrogen). Desalting was performed on Bio-Gel P chromatography columns (Bio-Rad).

Protein methods

Protein content was measured after Bradford [20], utilizing BSA as a standard.

Cell-free extracts and purified proteins were analyzed electrophoretically by SDS–PAGE according to [21]. Coomassie brilliant blue was used to stain protein bands. Western blotting was performed after standard techniques [22]. Proteins in the gel were blotted onto PVDF membranes using a Mini-ProteanII (Bio-Rad) apparatus. The membrane was blocked overnight at 4 °C, subsequently incubated with primary antibody at room temperature for 1 h, and then incubated with a HRP-conjugated anti-rabbit secondary antibody for 1 h. Detection was carried out with 3,3′-diaminobenzidine and hydrogen peroxide (Sigma) in 50 mM Tris–HCl, pH 8.0, 150 mM NaCl.

Reduction of disulfides by the EhTRXR/TRX system

Disulfide reduction was followed by means of a coupled assay system where, in the first reaction, *Eh*TRX8 or *Eh*TRX41 is reduced by *Eh*TRXR and NADPH. After the enzymatic reaction has run to completion, the disulfide (RSSR) is reduced by the respective TRX. Thus, disulfide reductase activity was determined by monitoring, at 30°C, the oxidation of NADPH at 340 nm in a reaction mixture (final volume of 250 μl) containing 50 mM potassium phosphate, pH 7.0, 2 mM EDTA, 300 μM NADPH, 1 μM *Eh*TRXR, 0–10 μM *Eh*TRX8 or *Eh*TRX41, and the different RSSR: 0–350 μM bovine insulin, 0–2000 μM oxidized glutathione (GSSG), 0–2000 μM cystine, or 0–200 μM oxidized trypanothione (TS_2).

Eh2CysPrx assay and kinetic analysis

*Eh*2CysPrx activity was measured by monitoring the NADPH oxidation at 340 nm and 30 °C. The standard assay mixture contained (in a final volume of 250 μl) 50 mM potassium phosphate, pH 7.0, 2 mM EDTA, 300 μM NADPH, 2 μM *Eh*TRXR, 20 μM *Eh*TRX8 or *Eh*TRX41, 1 μM *Eh*2CysPrx, and 500 μM *t*-bOOH. For kinetic analysis, the assay was performed using 0–500 μM *t*-bOOH and 0–30 μM *Eh*TRX8 or *Eh*TRX41.

The kinetic data were plotted as initial velocity (μM min^{-1}) versus substrate concentration. The kinetic parameters were acquired by fitting the data with a nonlinear least-squares formula and the Michaelis-Menten equation using the program Origin. Kinetic constants are the mean of at least three independent sets of data, and they are reproducible within ±10%.

Determination of redox potential of TRXs

Redox potential for TRXs was determined by following changes in the absorbance at 340 nm and 30°C. *Eh*TRX8 or *Eh*TRX41 (5–30 μM) was mixed with 36 μM NADPH in a total volume of 250 μl of 50 mM potassium phosphate, pH 7.0, 2 mM EDTA, followed by the addition first of 1 μM *Eh*TRXR and then an excess of $NADP^+$ (1.2 mM) as described previously [23]. Redox potentials were calculated according to the Nernst equation, based in the reactants concentration in the equilibrium. A value of −320 mV was used as redox potential of NADPH.

Confocal laser scanning microscopy

Cells culture were chilled for 15 min to detach trophozoites, harvested by centrifugation at 500 *g* at room temperature for 10 min, and washed twice with phosphate-buffered saline, PBS (8 g/L NaCl, 0.2 g/L KCl, 1.44 g/L Na_2HPO_4, 0.24 g/L KH_2PO_4, pH 7.4), to remove residual medium components. The cells were fixed with 4% paraformaldehyde and permeabilized for 1 h at room temperature in PBS, 0.05% Triton X-100, and 3% BSA. The cells were then incubated for 1 h at 37 °C with rabbit polyclonal antibodies against *Eh*TRXR or *Eh*TRX41 diluted 1:100 in PBS, 0.01% Triton X-100, and 1% BSA, followed by goat anti-rabbit secondary antibody labeled with fluorescein isothiocyanate (FITC) (final dilution of 1:1000; ICN Biomedicals) for 1 h at 37 °C.

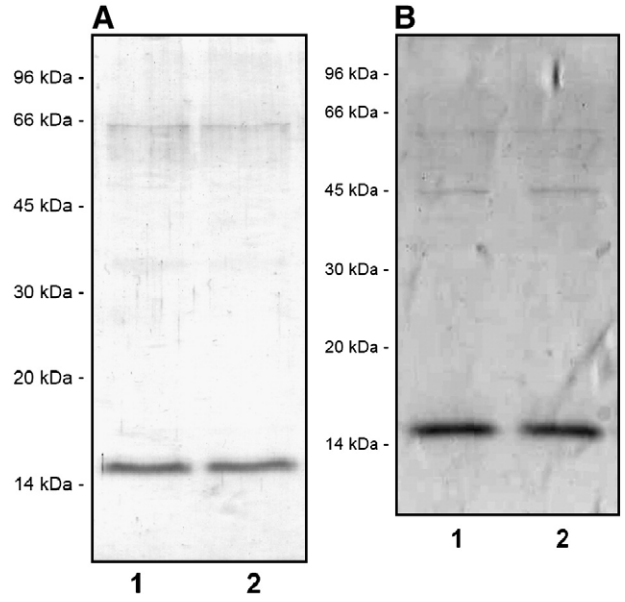

Fig. 1. (A) Electrophoretic analysis of the purified recombinant proteins. The proteins were defined by 15% (w/v) SDS–PAGE and stained with Coomassie blue. Lane 1, *Eh*TRX41; lane 2, *Eh*TRX8. (B) Western blotting. Lane 1, recombinant *Eh*TRX41; lane 2, recombinant *Eh*TRX8; the latter two were revealed with rabbit polyclonal anti-*Eh*TRX41.

Confocal images were collected using a Zeiss LSM5 Pascal laser-scanning confocal microscope equipped with an argon/helium/neon laser and a 100x (numerical aperture = 1.4) oil immersion objective (Zeiss Plan-Apochromat). Twenty to thirty-five confocal sections of 0.5 μm were taken parallel to the coverslip (*z* sections). Images were acquired using a Zeiss charge-coupled device camera and processed with LSM and Image J software. Three-dimensional deconvolution was performed with Autodeblur v9.3 software. Maximum intensities of 5 to 7 *z* sections were projected into images that depict 3–4 μm of the total *Z*-stack. Primary antibodies were prepared as described previously [12].

Results

Molecular cloning and expression of the ehtrx8 gene

The redox metabolism that is operative in *E. histolytica* has been recently revisited, after coming across the occurrence and functionality of *Eh*TRXR and one TRX (*Eh*TRX41) [12]. To further advance the characterization of molecular components able to interact with the reductase in vivo, we performed the molecular cloning of a gene putatively coding for another TRX (*Eh*TRX8) that is found (CDS 8. m00422) in the spliced nucleotide sequence of the parasite genome. The strategy for cloning and expression was similar to that previously employed for *Eh*TRX41. The full-length DNA fragment of the *ehtrx8* gene was amplified by PCR and inserted onto cloning (pGEM-T Easy) and expression (pRSET-A) vectors, as described under Materials and methods. The correctness of the amplified gene was verified by complete sequencing. The gene encodes for a 103-amino acid protein having a calculated *p*I of 5.3 and 11.6-kDa molecular mass.

After cloning of the gene onto the pRSET-A vector and transformation of *E. coli* BL21(DE3) cells, the recombinant *Eh*TRX8 protein could be expressed in a soluble form and conveniently purified by a single Co^{2+}-affinity chromatography step (Fig. 1). As shown, the *Eh*TRX8 recombinant protein visualized as a major protein band in SDS-PAGE (Fig. 1A) could also be revealed by using polyclonal antibodies raised against *Eh*TRX41 in Western blot experiments (Fig. 1B). This immunological cross-reactivity between both TRXs is coherent with the identity of 46.2% evidenced after the amino acid alignment of the proteins (see Fig. 1 in supplemental data). *Eh*TRX8 was also very similar to *Eh*TRX41 with respect to its kinetic behavior. Indeed, *Eh*TRXR quite similarly catalyzed the NADPH-dependent reduction of *Eh*TRX8 as determined by the insulin assay and by the method coupled to *Eh*2CysPrx to detoxify hydroperoxides [12] (see kinetic data in Table 1). Thus, results suggest that the redox system recently described in *E. histolytica* [12] could be operative with either of the TRXs, with *Eh*TRX8 being a component alternative to *Eh*TRX41 to function together with *Eh*TRXR.

Table 1
Kinetic parameters of *Eh*TRXR and *Eh*2CysPrx for the reduction/oxidation of *Eh*TRXs

Enzyme	Substrate	K_m (μM)	k_{cat} (min^{-1})	$k_{cat}\,K_m^{-1}$ ($M^{-1}\,s^{-1}$)
*Eh*TRXR	*Eh*TRX8	2.8	85.7	$5.10 \cdot 10^5$
	EhTRX41	3.6	130.0	$6.00 \cdot 10^5$
*Eh*2CysPrx	*Eh*TRX8	3.8	46.5	$2.04 \cdot 10^5$
	t-bOOH (+*Eh*TRX8)*	34.6	46.5	$2.22 \cdot 10^4$
	*Eh*TRX41	3.1	57.7	$3.10 \cdot 10^5$
	t-bOOH (+*Eh*TRX41)*	35.6	57.7	$2.70 \cdot 10^4$

Experimental conditions are detailed under Materials and methods.
* Specify the cosubstrates utilized for *t*-bOOH reduction.

Redox capacity of the EhTRXR/TRX system

To better evaluate the capacity of the redox system present in *E. histolytica* involving TRXR, we determined the redox potential of *Eh*TRX8 and *Eh*TRX41 following the approach recently utilized by Cheng et al. [23] for a similar system from *Drosophila melanogaster*. As shown in Fig. 2, the reaction between oxidized *Eh*TRX and NADPH, catalyzed by *Eh*TRXR, was found reversible:

$$NADPH + H^+ + TRX - S_2 \overset{TRXR}{\longleftrightarrow} NADP^+ + TRX - (SH)_2. \quad (1)$$

By performing the reaction with variable amounts of *Eh*TRX8 or *Eh*TRX41, we measured different concentrations of reactants and products at equilibrium. With these data, and utilizing the Nernst equation:

$$E^{\circ\prime}{}_{TRX} = E^{\circ\prime}{}_{NADPH} - \frac{R \cdot T}{n \cdot F} \cdot \ln \frac{[NADP^+][TRX - (SH)_2]}{[NADPH][TRX - S_2]}. \quad (2)$$

$E^{\circ\prime}$values of -286 and -283 mV were calculated for *Eh*TRX8 and *Eh*TRX41, respectively (see Table 1 in supplemental data). These values are similar to those reported for TRX from different organisms [18,24]. Also, the potential found for the proteins from *E. histolytica* suggests

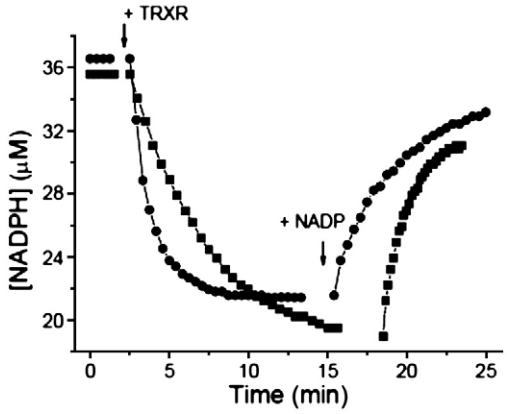

Fig. 2. Determination of redox potential of *Eh*TRXs. Reduction of disulfide in 15 μM ■ *Eh*TRX41 or ● *Eh*TRX8 was started by addition of 1 μM *Eh*TRXR. When the reaction had stopped, NADP was added to a final concentration of 1.2 mM. The formation of NADP and NADPH was followed by spectrophotometry at 340 nm.

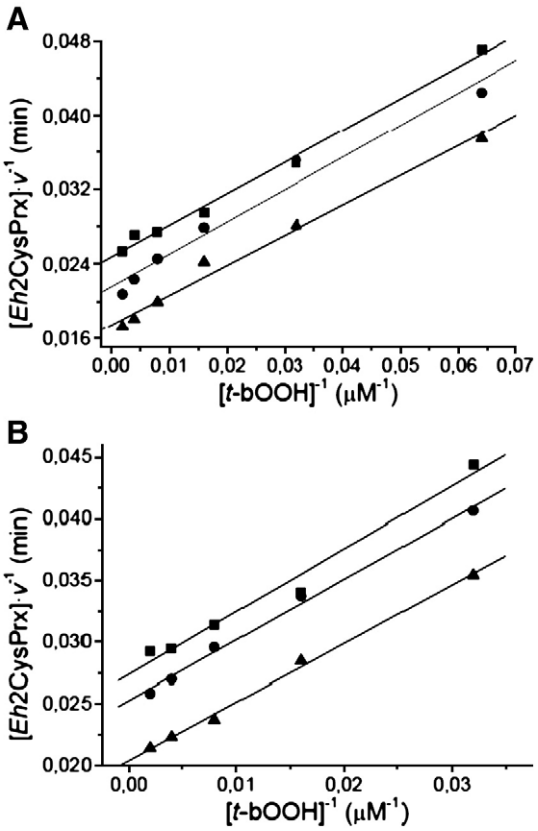

Fig. 3. Kinetic analysis of *Eh*2CysPrx. The reactions were performed in 50 mM buffer phosphate, pH 7.0, 2 mM EDTA, 300 μM NADPH, 2 μM *Eh*TRXR, 1 μM *Eh*2CysPrx, 0–500 μM *t*-bOOH, and different concentrations of *Eh*TRX8 (A) or *Eh*TRX41 (B): ■ 5; ● 10 and ▲ 20 μM.

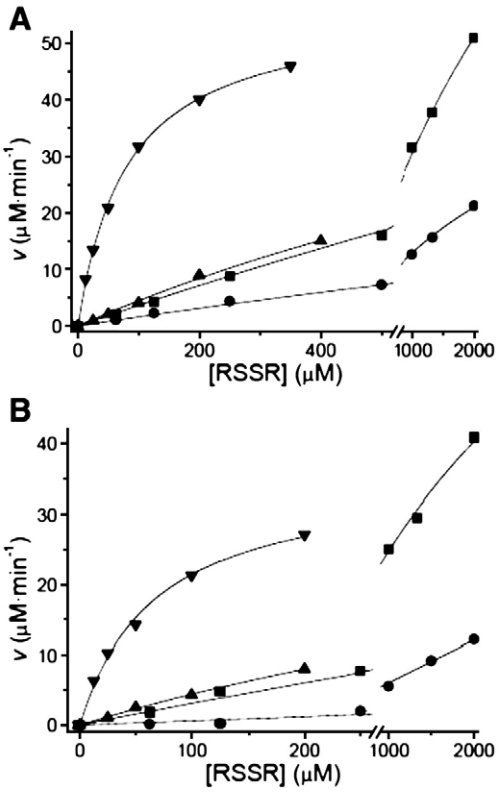

Fig. 4. Disulfide reduction by *Eh*TRXs enzymatically reduced. The reactions were performed in 50 mM buffer phosphate, pH 7.0, 2 mM EDTA, 300 μM NADPH, 1 μM *Eh*TRXR, 5 μM *Eh*TRX8 (A) or 5 μM *Eh*TRX41 (B) and different disulfides: ■, cystine; ●, glutathione; ▲, trypanothione; and ▼, insulin.

that either of these TRXs could be playing a key role in the redox metabolism of the parasite, being involved in the interchange of reducing equivalents with different metabolites. In this way, the *EhTRXR/TRX* system could be operative not only working together with *Eh*2CysPrx to detoxify hydroperoxides, as previously reported [12], but also has the appropriate redox potential to interact with other low molecular weight thiol compounds.

Peroxidase activity of Eh2CysPrx coupled to EhTRX

*Eh*2CysPrx was tested for hydroperoxide reducing activity coupled to the *Eh*TRXR/TRX system [12]. In these assays, the *Eh*TRXR was added in excess to assure that the different amounts of *Eh*TRX8 or *Eh*TRX41 were reduced to serve as the substrate affording reducing equivalents to *Eh*2CysPrx. The amoebic peroxidase exhibited Michaelis-Menten saturation kinetics regarding the different substrates, *t*-bOOH, *Eh*TRX8, and *Eh*TRX41. Double reciprocal plots for initial velocities with variable concentrations of *Eh*TRX8 (Fig. 3A) or *Eh*TRX41 (Fig. 3B) at different fixed values of *t*-bOOH yielding parallel lines indicate that the enzyme follows a ping-pong mechanism, in agreement with the kinetic pattern found for other peroxiredoxins [25–29]. The kinetic parameters for the recombinant *Eh*2CysPrx (obtained at saturating substrates concentration), summarized in Table 1, indicate that the enzyme displayed higher catalytic efficiency with respect to either TRXs than to *t*-bOOH, after the higher affinity it exhibited toward the former substrate.

Disulfides reduction assays

The *Eh*TRXR/TRX system was also analyzed in its ability to reduce disulfide compounds such as insulin, GSSG, cystine, and TS_2. Fig. 4 shows that the couple *Eh*TRXR/TRX transferred reducing equivalents from NADPH to the different disulfide compounds. The system operates with the reduction of *Eh*TRX8 (Fig. 4A) or *Eh*TRX41 (Fig. 4B) catalyzed by *Eh*TRXR (as shown in Eq. (1)), followed by the chemical redox interchange between the TRX and the respective disulfide:

$$TRX-(SH)_2+\mathrm{RSSR}\underset{k_{-2}}{\overset{k_2}{\leftrightarrow}}\mathrm{TRX}-S_2+2\,\mathrm{RSH}. \tag{3}$$

The rate of this spontaneous reaction is then established by the equation:

$$v=k_2\cdot[TRX-(SH)_2]\cdot[RSSR]. \tag{4}$$

As expected, in our hands the reaction was dependent on the concentration of the respective disulfide compound and also on levels of reduced *Eh*TRXs (Fig. 4). In the absence of TRX the different disulfides were not reduced by TRXR (see Figs. 2–5 in supplemental data). Second-order rate constants (k_2) summarized in Table 2 indicate

Table 2
Rate constants for the reduction of different disulfides by *Eh*TRXs

Disulfide	k (M^{-1} s^{-1})	
	*Eh*TRX8	*Eh*TRX41
Insulin	2435	2059
Cystine	124.7	110.7
GSSG	55.2	23.6
TS_2	118.6	143.0

The reaction mixtures contained 50 mM buffer phosphate, pH 7.0, 2 mM EDTA, 300 μM NADPH, 1 μM *Eh*TRXR, 0–350 μM insulin or 0–2000 μM cystine or 0–2000 μM glutathione or 0–200 μM trypanothione and different concentrations of *Eh*TRXs 0–10 μM at 30 °C.

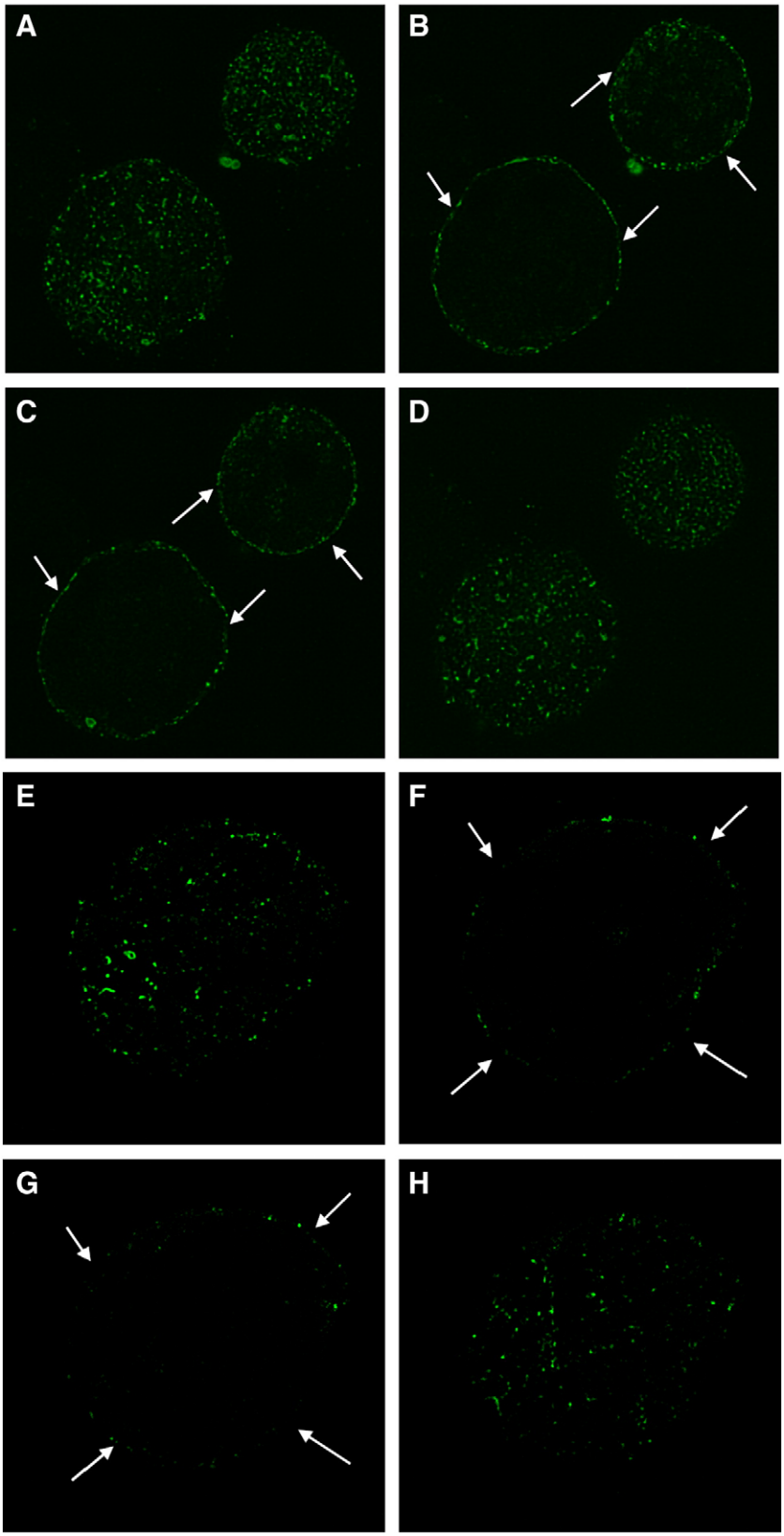

Fig. 5. Confocal laser scanning microscopy (CLSM) of *Entamoeba* cells using rabbit polyclonal anti-*Eh*TRXR (A–D) and anti-*Eh*TRX41 (E–H). CLSM pictures of the cellular localization of *Eh*TRXR and *Eh*TRX41 in *E. histolytica* (strain HM1-IMSS) trophozoites show intense labeling of the plasma membranes (arrows) at different optical section plains from the surface. *Eh*TRXR: (A) 0–4 μm, (B) 4–8 μm, (C) 8–12 μm, and (D) 12–16 μm. *Eh*TRX41: (E) 0–3 μm, (F) 3–6 μm, (G) 6–9 μm, and (H) 9–12 μm. Negative control using the conjugate alone revealed no staining (not shown).

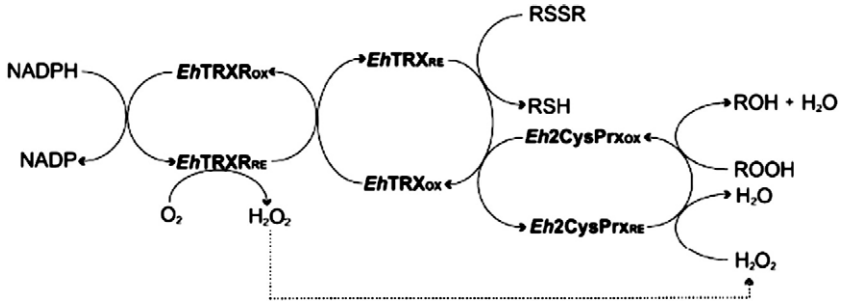

Fig. 6. Schematic description of the thioredoxin-linked hydroperoxide detoxification pathway in *E. histolytica*. ROOH (alkylhydroperoxide) and H_2O_2 (hydrogen peroxide).

that reduced *Eh*TRX8 or *Eh*TRX41 exhibited the highest capacity to reduce insulin (reaction performed as a control), and the lowest for GSSG, with two order of magnitude difference. The kinetic values for TS_2 and cystine were intermediate and differing 10-fold with respect to the formers.

Cellular localization of the EhTRXR/TRX system

The occurrence of *Eh*TRXR and *Eh*TRX41 in *E. histolytica* was already confirmed by Western blotting utilizing specific polyclonal antibodies, as recently reported by Arias et al. [12]. The antibodies were also useful to swot up the cellular localization of the proteins by immunofluorescence, with results illustrated in Fig. 5. Despite the fact that the nucleotide sequences of TRX41 and TRXR include no coding regions for any signal peptide or transmembrane hydrophobic domain, they seem to localize underlying the plasma membrane. As revealed by images in Fig. 5, a punctuated fluorescence was observed at the superior (Fig. 5A) or inferior (Fig. 5D) scrutiny of the cell. This pattern became fluorescent rings, adjacent to the cell periphery (Figs. 5B and C), when views were taken at different depths of the cell structure. The lack of signal displayed inside the cell (Figs. 5B and C) speaks in favor of a unique and particular localization of TRXR in the surrounding of the plasma membrane. Identical localization can be attributed to TRX 41 (and eventually to TRX 8), after similar immunofluorescence images were obtained by confocal microscopy using anti-TRX41 serum (Figs. 5E–H).

Discussion

E. histolytica, associated with poverty, ignorance, conditions of poor sanitation, and malnutrition, is the aetiological agent of a major public health problem worldwide. The increase in reports dealing with drug-resistant cases during amoebiasis treatment [4,5] reveals the value of in-depth characterization of metabolic pathways for rational design of new therapeutic agents. We have recently demonstrated the occurrence in *E. histolytica* of TRX and a reductase linked to its metabolic involvement [12]. This finding afforded a new understanding of the redox metabolism in the parasite, and the complete characterization of the molecules involved is a matter of interest. Results in the present work further advance in the knowledge of the redox metabolic scenario operating in *E. histolytica*, reaching the view depicted in Fig. 6. This scenario includes the involvement of *Eh*TRXR and *Eh*TRX41 (now also *Eh*TRX8, as an alternative) in a system functioning with *Eh*2CysPrx to detoxify hydroperoxides as well as reducing low molecular weight disulfides to maintain a redox balance in the parasite cytosol.

We previously purified recombinant *Eh*TRXR and *Eh*TRX41 to in vitro reconstitute a system probed to be functional working together with *Eh*2CysPrx in detoxifying hydroperoxides [12]. To reach a closer insight on the in vivo occurrence of the system, we utilized polyclonal antibodies raised against *Eh*TRXR and *Eh*TRX41 to localize both proteins at the cellular level. The TRXR/TRX system appears to prevail underlying the plasma membrane of *E. histolytica*, as it was illustrated by confocal laser scanning microscopy studies performed in the present work. This cellular localization reinforces the potential in vivo functionality of the ROS detoxification system, specially considering that *Eh*2CysPrx was previously identified also as an enzyme with a ectoplasmic accumulation [30], which can appear at the surface as protein associated to an *N*-acetylgalactosamine lectin [30,31]. Under conditions of oxidative stress, the lectin may recruit the peroxiredoxin for antioxidant protection [31]. The presence of TRXR and TRX41 (might be also TRX8) together with the *Eh*2CysPrx can be associated with the antioxidant system functionality as illustrated in Fig. 6.

*Eh*2CysPrx had being originally named *Eh*p29 [32] and identified as a member of the peroxiredoxin family of proteins [33]. In a recent work, the outstanding role of *Eh*2CysPrx, both in trophozoites survival under oxidative stress conditions as well as in pathogenesis of amoebiasis, has been established [31]. This probed metabolic relevance makes necessary a more detailed study of the kinetic characteristics of the system. In the present work we determined that the reduction of hydorperoxides by *Eh*2CysPrx, associated with *Eh*TRXR and *Eh*TRX, exhibited hyperbolic saturation kinetics for both of the substrates, reduced *Eh*TRXs and *t*-bOOH. The enzyme reaction follows a ping-pong mechanism, a pattern that together with the kinetic parameters determined for both substrates is in good agreement with data reported for peroxiredoxin from other organisms [29,31,33,34]. To the best of our knowledge, this is the first time that *Eh*2CysPrx is kinetically characterized in *E. histolytica* as a component of a redox cascade.

Redox potentials for *Eh*TRX8 and *Eh*TRX41 were calculated to be -286 and -283 mV, respectively, which are in good agreement with those values found for this kind of protein from other sources [18,24]. The potential of either TRX is considerably more negative than those corresponding to low molecular weight disulfides reported as key redox metabolites. As expected, reduction equivalents from NADPH, primarily transferred to *Eh*TRXs by catalysis of *Eh*TRXR, could then be chemically driven to the reduction of cystine, TS_2, or GSSG. This result has a physiological significance after the possible role of the low molecular weight thiols generated in the described reaction. First, in *E. histolytica* cysteine was accounted as an important component of the antioxidant defense [15,16,35], and as the main intracellular thiol that can be synthesized de novo from sulfate [35,36]. Three nucleotide sequences encoding putative cysteine synthases can be found in the *E. histolytica* genome project (http://www.genedb.org; 3.m99156, 93.m00149, and 328.m00057). Interestingly, no evidence for the occurrence of a cystine reductase was found for this parasite, which gives additional value to the redox capacity of the *Eh*TRXR/TRX system.

Secondly, TS_2, initially described in trypanosomatids [37–40], is another disulfide that could be physiologically available in *E. histolytica* [8,11,14]. Besides that the occurrence of trypanothione in the parasite was critically questioned [14], no gene is found in the genome project for a reductase of the disulfide. Thus, if trypanothione actually is present in *E. histolytica*, its reduction should be associated

with TRX8 or TRX41. Additionally, glutathione is a necessary substrate in the synthesis of trypanothione and was found to occur at low concentrations in the parasite [14]. The absence of a glutathione reductase in *E. histolytica* [31] suggests that *Eh*TRXs could be functionally involved in the maintenance of glutathione at its reduced state in the parasite.

Concluding remarks

This work improves the knowledge about the reactions that, in *E. histolytica*, are managing the redox equivalents flux, which constitute a critical metabolic mechanism for the parasite survival and virulence. As schematized in Fig. 6, the *Eh*TRXR/TRX system appears as an important tool not only for hydroperoxide detoxification but also for maintaining in a reduced form other redox compounds. This more versatile functioning supports a view where the TRX-dependent system plays a relevant role in the parasite defense against oxygen toxicity during the oxidizing extraintestinal phase of the amoebic infection.

The relevance of the TRXR/TRX system in *E. histolytica* has been recently supported by a work showing how metronidazole, a drug usually used in the treatment of amoebiasis, can bind to TRXR and TRX (between other protein thiols) to form inactive adducts [41]. Thus, the lack of an active TRXR decreases levels of reduced TRX and consequently of the peroxiredoxin, making the cells more sensitive to oxygen in the presence of metronidazole due to a reduced capability of the cells to detoxify ROS [41]. Outstandingly, in the scenario depicted in Fig. 6, an increase in oxygen levels (as expected during the exposure of the parasite in the blood stream phase) triggers the NADPH oxidase activity of the TRXR [12], which generates H_2O_2. This toxic compound can be further metabolized by peroxiredoxin associated with the *Eh*TRXR/TRX system. Thus, any impairment caused on the *Eh*TRXR/TRX system (as in the case of metronidazole [41]) should dramatically affect the parasite survival. In this framework, the *Eh*TRXR can be considered as a key target for the development of new chemotherapeutic agents. This view is reinforced by data detailed in Fig. 6 of the supplemental data, illustrating a high dissimilarity in structure between the enzyme from *Entamoeba* and those reductases found in humans.

Acknowledgments

This work was supported by grants from ANPCyT (PICT′03, 1-14733; PAV′03, 137, PICT′03 05-13469), CONICET (PIP 6358), UNL (CAI+D 2006), and Howard Hughes Medical Institute. We thank Rodrigo Quiroga for helpful support in confocal laser scanning microscopy. D.G.A. and P.G.C. are fellows from CONICET (Argentina) and H.D.L., A.A.I., and S.A.G. are investigator career members from the same institution.

Appendix A. Supplementary data

Supplementary data associated with this article can be found, in the online version, at doi:10.1016/j.freeradbiomed.2008.03.008.

References

[1] Bhattacharya, A.; Satish, S.; Bagchi, A.; Bhattacharya, S. The genome of *Entamoeba histolytica*. *Int. J. Parasitol.* **30:**401–410; 2000.
[2] Davis, A. N.; Haque, R.; Petri Jr., W. A. Update on protozoan parasites of the intestine. *Curr. Opin. Gastroenterol.* **18:**10–14; 2002.
[3] Stanley Jr., S. L. Amoebiasis. *Lancet* **361:**1025–1034; 2003.
[4] Bansal, D.; Malla, N.; Mahajan, R. C. Drug resistance in amoebiasis. *Indian J. Med. Res.* **123:**115–118; 2006.
[5] Bansal, D.; Sehgal, R.; Chawla, Y.; Malla, N.; Mahajan, R. C. Multidrug resistance in amoebiasis patients. *Indian J. Med. Res.* **124:**189–194; 2006.
[6] Ali, V.; Nozaki, T. Current therapeutics, their problems, and sulfur-containing-amino-acid metabolism as a novel target against infections by "amitochondriate" protozoan parasites. *Clin. Microbiol. Rev.* **20:**164–187; 2007.
[7] Krauth-Siegel, R. L.; Bauer, H.; Schirmer, R. H. Dithiol proteins as guardians of the intracellular redox milieu in parasites: old and new drug targets in trypanosomes and malaria-causing plasmodia. *Angew. Chem. Int. Ed. Engl.* **44:**690–715; 2005.
[8] Ondarza, R. N.; Hurtado, G.; Iturbe, A.; Hernandez, E.; Tamayo, E.; Woolery, M. Identification of trypanothione from the human pathogen *Entamoeba histolytica* by mass spectrometry and chemical analysis. *Biotechnol. Appl. Biochem.* **42:**175–181; 2005.
[9] Ondarza, R. N.; Hurtado, G.; Tamayo, E.; Iturbe, A.; Hernandez, E. Naegleria fowleri: a free-living highly pathogenic amoeba contains trypanothione/trypanothione reductase and glutathione/glutathione reductase systems. *Exp. Parasitol.* **114:**141–146; 2006.
[10] Schmidt, A.; Krauth-Siegel, R. L. Enzymes of the trypanothione metabolism as targets for antitrypanosomal drug development. *Curr. Top. Med. Chem.* **2:**1239–1259; 2002.
[11] Tamayo, E. M.; Iturbe, A.; Hernandez, E.; Hurtado, G.; de Lourdes Gutierrez, X. M.; Rosales, J. L.; Woolery, M.; Ondarza, R. N. Trypanothione reductase from the human parasite *Entamoeba histolytica*: a new drug target. *Biotechnol. Appl. Biochem.* **41:**105–115; 2005.
[12] Arias, D. G.; Gutierrez, C. E.; Iglesias, A. A.; Guerrero, S. A. Thioredoxin-linked metabolism in *Entamoeba histolytica*. *Free Radic. Biol. Med.* **42:**1496–1505; 2007.
[13] Loftus, B.; Anderson, I.; Davies, R.; Alsmark, U. C.; Samuelson, J.; Amedeo, P.; Roncaglia, P.; Berriman, M.; Hirt, R. P.; Mann, B. J.; Nozaki, T.; Suh, B.; Pop, M.; Duchene, M.; Ackers, J.; Tannich, E.; Leippe, M.; Hofer, M.; Bruchhaus, I.; Willhoeft, U.; Bhattacharya, A.; Chillingworth, T.; Churcher, C.; Hance, Z.; Harris, B.; Harris, D.; Jagels, K.; Moule, S.; Mungall, K.; Ormond, D.; Squares, R.; Whitehead, S.; Quail, M. A.; Rabbinowitsch, E.; Norbertczak, H.; Price, C.; Wang, Z.; Guillen, N.; Gilchrist, C.; Stroup, S. E.; Bhattacharya, S.; Lohia, A.; Foster, P. G.; Sicheritz-Ponten, T.; Weber, C.; Singh, U.; Mukherjee, C.; El-Sayed, N. M.; Petri Jr., W. A.; Clark, C. G.; Embley, T. M.; Barrell, B.; Fraser, C. M.; Hall, N. The genome of the protist parasite *Entamoeba histolytica*. *Nature* **433:**865–868; 2005.
[14] Ariyanayagam, M. R.; Fairlamb, A. H. *Entamoeba histolytica* lacks trypanothione metabolism. *Mol. Biochem. Parasitol.* **103:**61–69; 1999.
[15] Mehlotra, R. K. Parasitic protozoa: thiol-based redox metabolism. *Trends Parasitol.* **20:**58–59; 2004.
[16] Tekwani, B. L.; Mehlotra, R. K. Molecular basis of defence against oxidative stress in *Entamoeba histolytica* and *Giardia lamblia*. *Microbes Infect.* **1:**385–394; 1999.
[17] Loftus, B. J.; Hall, N. *Entamoeba*: still more to be learned from the genome. *Trends Parasitol.* **21:**453; 2005.
[18] Schmidt, H.; Krauth-Siegel, R. L. Functional and physicochemical characterization of the thioredoxin system in Trypanosoma brucei. *J. Biol. Chem.* **278:**46329–46336; 2003.
[19] Diamond, L. S.; Harlow, D. R.; Cunnick, C. C. A new medium for the axenic cultivation of *Entamoeba histolytica* and other *Entamoeba*. *Trans. R. Soc. Trop. Med. Hyg.* **72:**431–432; 1978.
[20] Bradford, M. M. A rapid and sensitive method for the quantitation of microgram quantities of protein utilizing the principle of protein-dye binding. *Anal. Biochem.* **72:**248–254; 1976.
[21] Laemmli, U. K. Cleavage of structural proteins during the assembly of the head of bacteriophage T4. *Nature* **227:**680–685; 1970.
[22] Maniatis, T. F.; Fritsch, E. F.; Sambrook, J. Molecular cloning: a laboratory manual. Cold Spring Harbor Laboratory, Cold Spring Harbor, NY; 1982.
[23] Cheng, Z.; Arscott, L. D.; Ballou, D. P.; Williams Jr., C. H. The relationship of the redox potentials of thioredoxin and thioredoxin reductase from Drosophila melanogaster to the enzymatic mechanism: reduced thioredoxin is the reductant of glutathione in Drosophila. *Biochemistry* **46:**7875–7885; 2007.
[24] Forman, H. J.; Fukuto, J.; Torres, M. Signal transduction by reactive oxygen and nitrogen species: pathways and chemical principles. Kluwer Academic, Netherlands; 2003.
[25] Montemartini, M.; Nogoceke, E.; Gommel, D. U.; Singh, M.; Kalisz, H. M.; Steinert, P.; Flohe, L. Tryparedoxin and tryparedoxin peroxidase. *BioFactors* **11:**71–72; 2000.
[26] Montemartini, M.; Nogoceke, E.; Singh, M.; Steinert, P.; Flohe, L.; Kalisz, H. M. Sequence analysis of the tryparedoxin peroxidase gene from *Crithidia fasciculata* and its functional expression in *Escherichia coli*. *J. Biol. Chem.* **273:**4864–4871; 1998.
[27] Montemartini, M.; Kalisz, H. M.; Hecht, H. J.; Steinert, P.; Flohe, L. Activation of active-site cysteine residues in the peroxiredoxin-type tryparedoxin peroxidase of *Crithidia fasciculata*. *Eur. J. Biochem.* **264:**516–524; 1999.
[28] Lopez, J. A.; Carvalho, T. U.; de Souza, W.; Flohe, L.; Guerrero, S. A.; Montemartini, M.; Kalisz, H. M.; Nogoceke, E.; Singh, M.; Alves, M. J.; Colli, W. Evidence for a trypanothione-dependent peroxidase system in *Trypanosoma cruzi*. *Free Radic. Biol. Med.* **28:**767–772; 2000.
[29] Guerrero, S. A.; Lopez, J. A.; Steinert, P.; Montemartini, M.; Kalisz, H. M.; Colli, W.; Singh, M.; Alves, M. J.; Flohe, L. His-tagged tryparedoxin peroxidase of *Trypanosoma cruzi* as a tool for drug screening. *Appl. Microbiol. Biotechnol.* **53:**410–414; 2000.
[30] Hughes, M. A.; Lee, C. W.; Holm, C. F.; Ghosh, S.; Mills, A.; Lockhart, L. A.; Reed, S. L.; Mann, B. J. Identification of *Entamoeba histolytica* thiol-specific antioxidant as a GalNAc lectin-associated protein. *Mol. Biochem. Parasitol.* **127:**113–120; 2003.
[31] Sen, A.; Chatterjee, N. S.; Akbar, M. A.; Nandi, N.; Das, P. The 29-kilodalton thiol-dependent peroxidase of *Entamoeba histolytica* is a factor involved in pathogenesis and survival of the parasite during oxidative stress. *Eukaryot. Cell* **6:**664–673; 2007.
[32] Bruchhaus, I.; Richter, S.; Tannich, E. Removal of hydrogen peroxide by the 29 kDa protein of *Entamoeba histolytica*. *Biochem. J.* **326** (Pt 3)**:**785–789; 1997.

[33] Hofmann, B.; Hecht, H. J.; Flohe, L. Peroxiredoxins. *Biol. Chem.* **383:**347–364; 2002.
[34] Akerman, S. E.; Muller, S. Peroxiredoxin-linked detoxification of hydroperoxides in Toxoplasma gondii. *J. Biol. Chem.* **280:**564–570; 2005.
[35] Nozaki, T.; Ali, V.; Tokoro, M. Sulfur-containing amino acid metabolism in parasitic protozoa. *Adv. Parasitol.* **60:**1–99; 2005.
[36] Krishna, C.; Jain, R.; Kashav, T.; Wadhwa, D.; Alam, N.; Gourinath, S. Crystallization and preliminary crystallographic analysis of cysteine synthase from *Entamoeba histolytica*. *Acta Crystallogr. Sect. F: Struct. Biol. Cryst. Commun.* **63:**512–515; 2007.
[37] Fairlamb, A. H.; Blackburn, P.; Ulrich, P.; Chait, B. T.; Cerami, A. Trypanothione: a novel bis(glutathionyl)spermidine cofactor for glutathione reductase in trypanosomatids. *Science* **227:**1485–1487; 1985.
[38] Fairlamb, A. H.; Henderson, G. B.; Cerami, A. The biosynthesis of trypanothione and N1-glutathionylspermidine in *Crithidia fasciculata*. *Mol. Biochem. Parasitol.* **21:**247–257; 1986.
[39] Fairlamb, A. H. The role of glutathionylspermidine and trypanothione in regulation of intracellular spermidine levels during growth of *Crithidia fasciculata*. *Adv. Exp. Med. Biol.* **250:**667–674; 1988.
[40] Henderson, G. B.; Yamaguchi, M.; Novoa, L.; Fairlamb, A. H.; Cerami, A. Biosynthesis of the trypanosomatid metabolite trypanothione: purification and characterization of trypanothione synthetase from *Crithidia fasciculata*. *Biochemistry* **29:**3924–3929; 1990.
[41] Leitsch, D.; Kolarich, D.; Wilson, I. B.; Altmann, F.; Duchene, M. Nitroimidazole action in *Entamoeba histolytica*: a central role for thioredoxin reductase. *PLoS Biol.* **5:**e211; 2007.